Analysis of Well Test NLW-GT-02

June 2018

Report G1340_4

Analysis of Welltest NLW-GT-02

G 1340_4 June 2018

Author
Pieter Lingen (plingen@worldonline.nl)

Reviewed by
Christiaan van der Harst – Chief RE

Prepared for
Trias Westland
Nieuweweg 1
2685 ZG Poeldijk
The Netherlands

Prepared by
PanTerra Geoconsultants B.V.
Weversbaan 1-3
2352 BZ Leiderdorp
The Netherlands
T +31 (0)71 581 35 05
F +31 (0)71 301 08 02
info@panterra.nl

Summary

- During the 33 hours test (with 9.5 hours of water production) of well Naaldwijk GT-02, starting 31 May 2018, the water production rates varied between 219 and 450 m^3/hr with a cumulative production of 2990 m^3.

- Evaluation of the test indicates an average reservoir permeability of about 800 mD if the entire 57 m thick reservoir contributes.
    - The observed permeability is the radial permeability. The average permeability between NLW-GT-02 and its doublet well might be higher because of placement parallel to the dominant fault structure. An interference test has therefore been set up during the test of this well by hanging pressure gauges in NLW-GT-01.

- Damage skin is 0.02, which indicates that there is no formation damage. The rate-dependent skin is 0.0022 hr/m^3 caused by friction in the vertical conduit between reservoir and gauge.

- The well test interpretation indicates the presence one flow barrier at a distance of 370 meters. This barrier is probably the boundary fault to the north-east, but does not have to be fully sealing (see Figure 1). The distance depends on the estimated compressibility.

- Static reservoir pressure at 2375 mtv is 240.6 bara.
- Reservoir temperature is about 87.5 °C.
- Transient flow capacity (PI) after 34 hours flow is about 21 m^3/hr/bar.
- The correction for the changing temperature of the water column between the ESP and BHP is similar as observed in NLW-GT-01, but with a slightly higher density. The continuing increase in pressure difference between the ESP and bottom gauges with the cooling of the water column indicates a water salinity of 130 kg/m^3 NaCl equivalent.

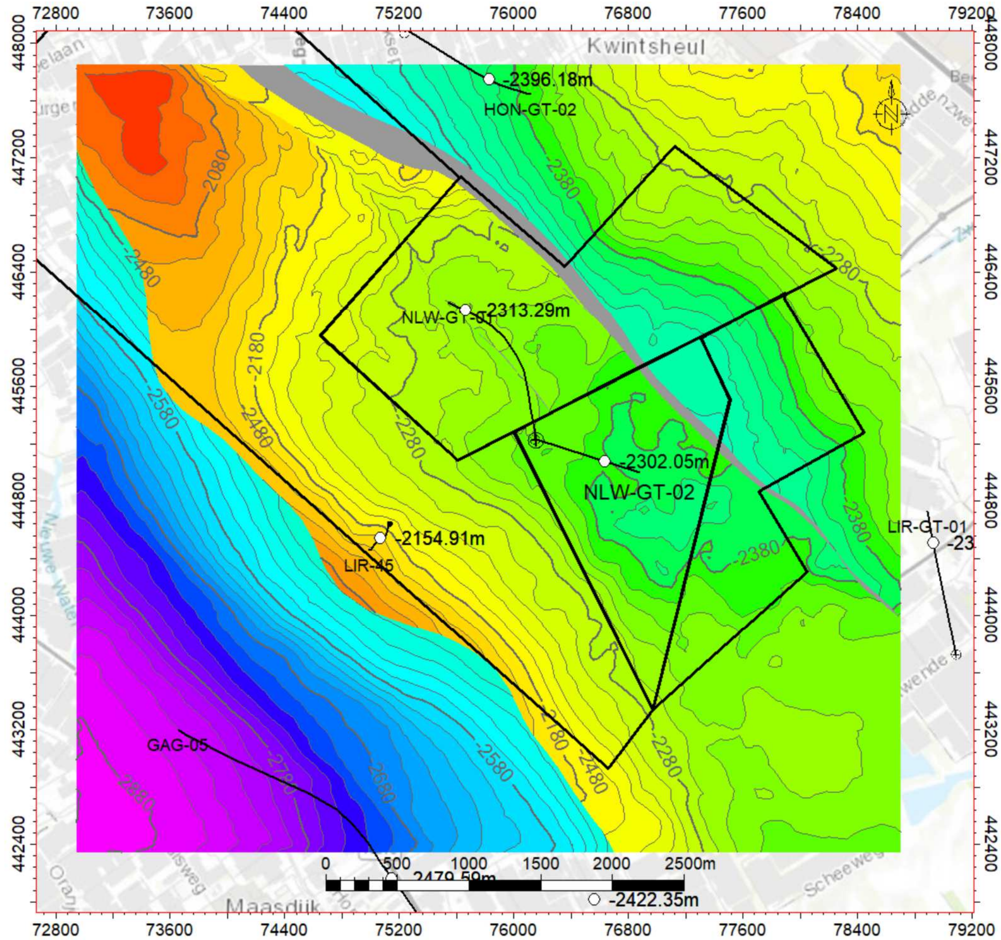

Figure 1 - Top Structure Map Delft sandstone (by T&A); Both Well NLW-GT-01 and well NLW-GT-02 are shown. Faults are represented by thick grey lines.

Results of Well test

Gegevens voor test interpretatie		Waarde	Dimensie
Naam van de put		NLW-GT-02	
Top aquifer		2460	m (langs boorgat)
“		2365	en m (TVD)
Basis aquifer		2578	m (langs boorgat)
“		2454	en m (TVD)
Netto dikte Aquifer		57	m (TVD)
Netto/bruto aquifer		64	%
Gemiddelde porositeit aquifer		18.7	%
Zoutgehalte formatiewater van sample		130	kg/m3
Verwachte max. temperatuur geproduceerde water[1]		87.5	ºC
Casing 20“		1076	m tv
Casing 13 5/8”		2295	m tv
Casing 9 5/8”		2516	m tv
Diameter boorgat bij aquifer		12,25 (9 5/8 casing)	Inch
Top productie-interval/filter (6 5/8 x 7”)		2451	m (langs boorgat)
“		2358	m (TVD)
Basis productie-interval/filter (6 5/8 x 7”)		2569	m (langs boorgat)
“		2444	m (TVD)
Weerstand over screens[2]		0	bar
Locatie pomp		721.7	m (ah)
Locatie meetsonde voor druk		737.1	m (tv)
Locatie diepe wireline gauge		2259.8	m (langs boorgat)
“		2197.1	m tv
Meetreeksen Puttest[4]		Eind ESP druk, bar	Eind Debiet, m3/uur
Flow 1		62.9	219
Flow 2		60.9	288
Flow 3		55.9	388
Flow 4		53.3	450
Flow 5		61.5	215
Flow 6		59.7	281
Flow 7		55.6	363
BU		68.9	0
Uitkomsten test interpretatie en analyses			
Total Skin		0.48- 0.81	
H		57	m
K		800	mD
KH		45.6	D*m
PI (transient 34 hrs)		21	m^3/hr/bar
One flow-barrier at approximately		370	m from well
Deviatie			
Diepte langs boorgat	Diepte m tv	East	North
0	0	76154	445230
	2365	551	-169
Mid reservoir	2390	576	-176
	2454	623	-191

[1] Deze temperatuur wordt als gemiddelde aquifer temperatuur beschouwd
[2] Geen meting van weerstand over filter

Contents

1 Introduction

The geothermal well NLW-GT-01 (Naaldwijk) was production tested for some 33 hours.
The test started 31/05/2018 14:55 with a multi-rate test for 9.5 hours, followed by a shut-in period of 23.5 hours.

The ESP generated production rates were increased in short steps from 223 to 450 m^3/hr, with a final longer flow period of 3.8 hours at 361 m^3/hr. Cumulative water produced was about 2980 m^3. The pressure and temperature data were recorded both by the ESP gauge at 737 mtv and two high-accuracy gauges on wireline at 2197 mtv.

The well was produced from the Delft sandstone, 2365 – 2454 mtv, covered by sand exclusion screens. The total net sand thickness is estimated at 57 m.

The correction formula, as determined from the ESP data in combination with the downhole gauge data, was used to determine the water salinity. During the build-up, 8 instances of wireline shrinkage have been observed. Although too small to have a significant effect on the analysis, they were removed and the deep gauge data have also been extrapolated to top good reservoir at 2375 mtv in order to have the best definition of the distance to the observed flow barrier.

2 Reservoir and Rate data

Most reservoir and fluid data have been left the same as in NLW-GT01: The average porosity of the two layers has been estimated at 18.7%. Net thickness is here 57 mtv.

The wellbore radius Rw has been set to the outer radius of the screens, or 0. 40 ft. In view of the deviation of the well with an average angle of about 40 degrees through the reservoir, the wellbore radius was adjusted to $Rw*\sqrt{\{(1+1/\cos\alpha^2)/2\}}$ = 0.47 ft, for the analysis with a vertical well model.

The reservoir temperature is estimated at 87.5 °C, the maximum observed BHP gauge temperature at the highest rate.

The water viscosity and water compressibility have been based on the salinity: µw = 0.433 cP and Cw = 2.5E-6 psi^{-1} respectively. A value of Cf = 3.5E-06 psi^{-1} was used for the pore compressibility.
The porosity and total compressibility (Cw + Cf) may have to be adjusted once the interference test with the first well is completed.

Table-1 lists the used rate sequence during the production test, as obtained from the rate data presented in Fig 1, chapter 3.

Table-1

Total time, hrs	Delta time, hrs	Flow rate m^3/hr	Flow Rate, b/d
0.575	0.58	219	33110
1.073	0.5	288	43400
1.345	0.27	388	58520
2.397	1.05	450	67910
4.672	2.28	215	32430
5.660	0.99	281	42480
9.454	3.79	363	54830

3 Recorded Pressures, BHP and ESP.

Fig-2 shows the original downhole gauges, together with the flowrates and temperatures. As both downhole gauges show practically the same pressures, only the bottom gauge has been used for analysis. As these gauges are just 178m above top reservoir, the cooling during the build-up is only relatively small (from 87.5 to 82.5 °C). The cooling effect at the ESP is more significant, declining from 87.1 to 60 °C.

The practice to record all data per second is leading to a very large data volume. As the early build-up is always disturbed by wellbore effects, 3 or 4 points per minute are sufficient for the analysis, reducing the time of data preparation. In the presented plots the data have been filtered and not more than 500 data points have been used to describe the whole test. These points still use all data by applying a moving-average filtering on the original data set.

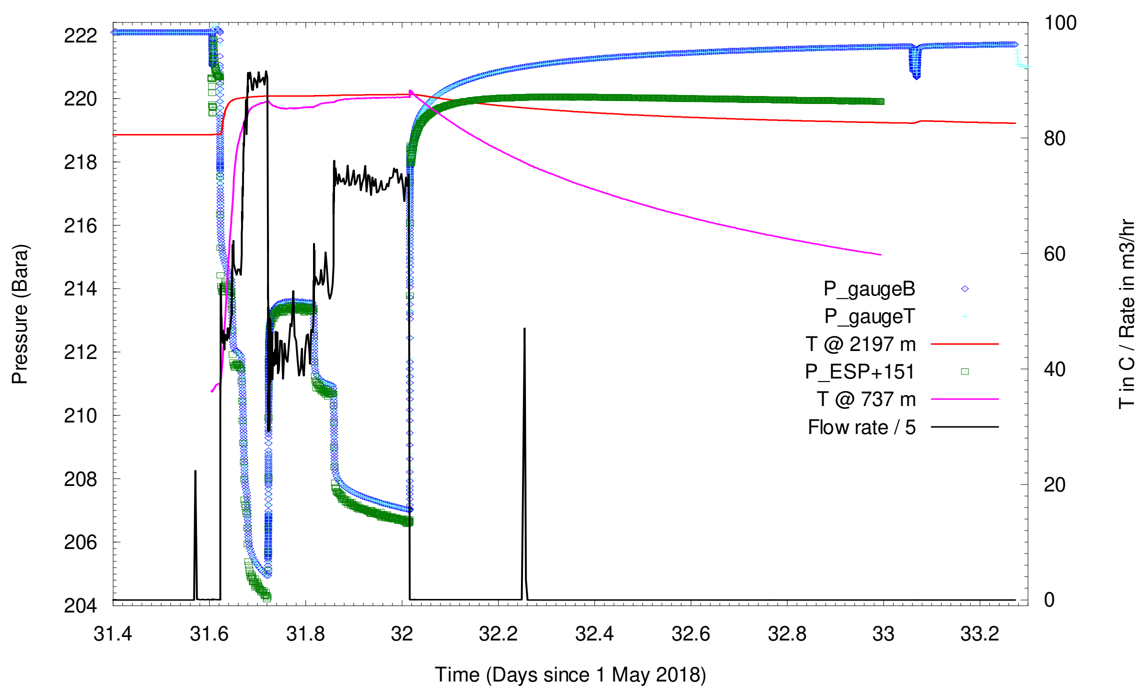

Figure 2 - Bottom Hole gauges plus ESP: pressures, temperatures and flowrates.

4 Corrections during build-up

The pressures of the downhole gauge were correlated with those of the ESP, 1460m higher, as function of the ESP temperature in Fig-3. The resulting correction formula, only matching ESP temperatures below 86 °C, is: DP = CDC*L*{1056.3+0.476*(87.5-T)-0.0034*(87.5-T)**2}

With DP the pressure correction, CDC a constant [CDC= 9.8063E-5 if pressure in bar] and L (= 1460) the distance in meters between ESP and bottom gauges, and T the current ESP gauge temperature in °C. With a maximum recorded BHP temperature of 87.5 °C, this maximum temperature was used in the equation shown above. This formula can thus be used to calculate BHP pressures from pressure data at ESP depth.

The blue points are the pressure differences between BHP and top gauge, with the fitted function through those points in red. The green points are the blue points minus the red fitted curve, plotted at the large right-hand scale. The inaccuracy is relatively small and caused by the limited resolution of the ESP gauge.

The function, displayed in Fig-3 and used to calculate the pressure difference between ESP depth and Bottom Hole depth, is very similar to that obtained from the test data of NLW-GT-01, but with a slightly higher density.

The water salinity was calculated from the pressure difference of 151.5 bar at an average column temperature of 85.2 °C. With a vertical distance of 1460m this gives a pressure gradient of 0.10376 bar/m, or 1058.1 kg/m3 which indicates a salinity of 130 kg/m3 NaCl equivalent {equivalent means that all the different salts (all metals can form salts) are translated to the amount of NaCl that gives the observed water density}, using the curves presented in Appendix 1, after subtraction of the correction for the reservoir pressure. Note that the salinity in NLW-GT-01 was 120 kg/m3.

The 8 small steps during the build-up are caused by shrinkage of the wireline and have been removed by adding the step size to all subsequent pressures, figure 4.

The green points are the observed deep gauge pressures with two corrections: for the gauge movement and using the density correction of Fig-3 for the cooling water column of 178 m between gauge and the top of the good quality reservoir.

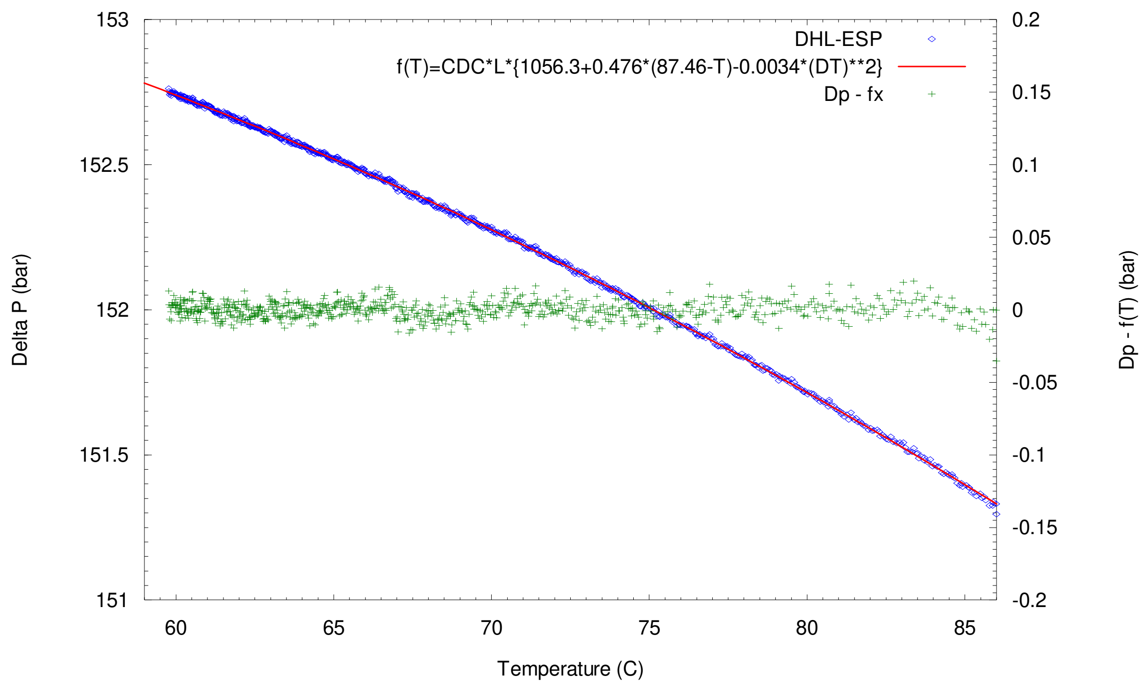

Figure 3 - Pressure correction to convert pressures at ESP depth to BHP as a function of Temperature.

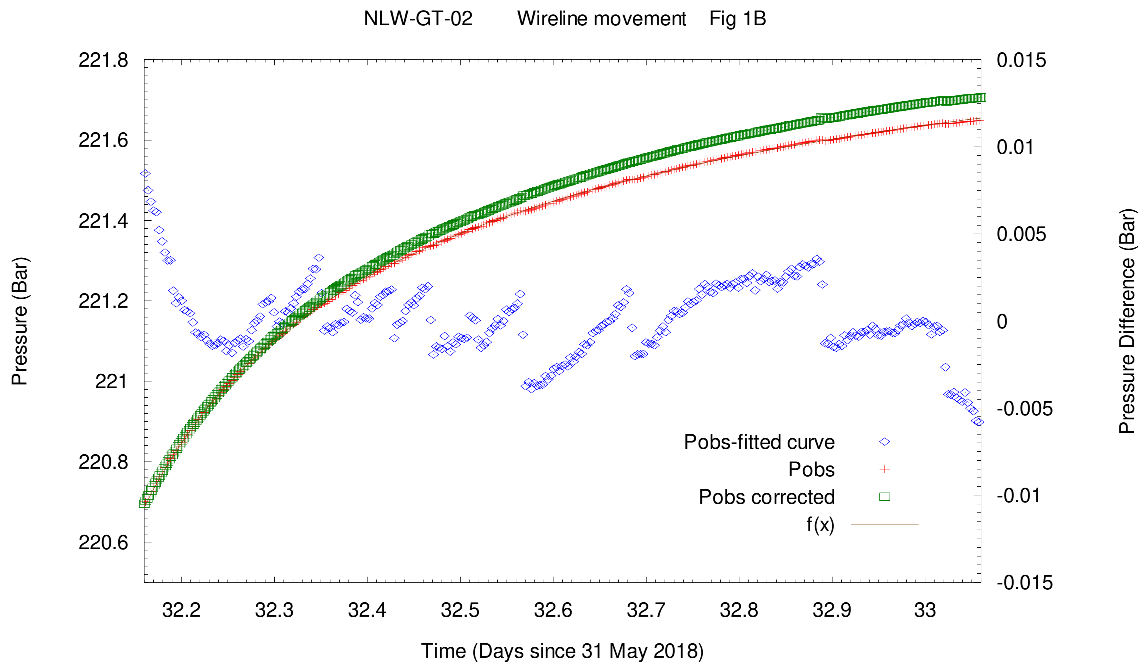

Figure 4 – Removal of pressure steps due to wireline shrinkage plus extrapolation to top reservoir.

5 Analysis method

The pressure test analysis is carried out by the match of the most appropriate analytical well/reservoir model response with the total test history. In this way, no approximations have to be used, as for the model response the flow equations are solved for the reported flow rates. It should be noted that each pressure point measured in a well depends on the total previous rate history of that well, both in the real reservoir as in the analytical model. Analysis of only one rate period, ignoring the rate history, can thus give only an approximation of the actual reservoir/well parameters.

The standard analysis results in a split of the observed productivity at reservoir depth (otherwise Tubing Head Pressure data would be sufficient) into the reservoir potential (k*h/µ) and an extra flow resistance, the skin, S. This skin is any deviation of the effective wellbore radius, rw, and represents formation damage of the reservoir, which may be caused by drilling (mud invasion), resistance over the sand exclusion screens, by deposits of evaporates, etc. Some forms of skin can be removed (e.g. by a well clean-out with coiled tubing, injection of acid or by temporary production at a high production rate). The skin includes also the flow resistance over the vertical conduit between reservoir and pressure gauge; this type of skin is rate dependent and can therefore be determined by testing with at least 3 different flow rates, so that the (rate independent) damage skin can be calculated.
The skin can also be negative as a result of acid stimulation (increased permeability just around the wellbore), fraccing or sand production (enlarging the effective wellbore radius).

From a detailed analysis of mainly the build-up pressure data, information about the presence and distance of flow barriers in the reservoir (faults, channel boundaries or sedimentological changes) can be obtained.

As no deviated well model is available, a vertical well model has been used, based on the assumption that the flow in the reservoir at some distance from the well will be horizontal and thus the same for a deviated and a vertical well. This is usually a valid assumption, as the vertical permeability is normally lower than the horizontal permeability in sandstone. The reservoir geometry shown by the top structure map in Fig-1 shows that there are parallel faults. The model-well can be placed in a rectangular bounded reservoir as indicated in the sketch below. As only one flow barrier is observed on the derivative of Fig-6, only one model has been matched with the data, obtained by setting X, Y and Xw at a very large value and only matching on Yw.

The matched-model response for early times usually deviates from the observed pressures. These early build-up pressures are expected to be influenced by water hammer, the latent motor heat of the ESP motor and possibly by cold-water fall-back. These temporary effects are hard to model in detail and have no impact on the estimation of reservoir properties.

The model response to the test rate history - including all flow and shut-in periods (even the pre-test flow periods for which no pressure data are available) - is obtained by the principle of super-position. The parameters of the model are varied until the difference between model response and observed well response is minimal.

The transient Productivity Index (PI) is obtained from the last point of the underlying single-rate model response and is the best estimate of the longer-term PI.

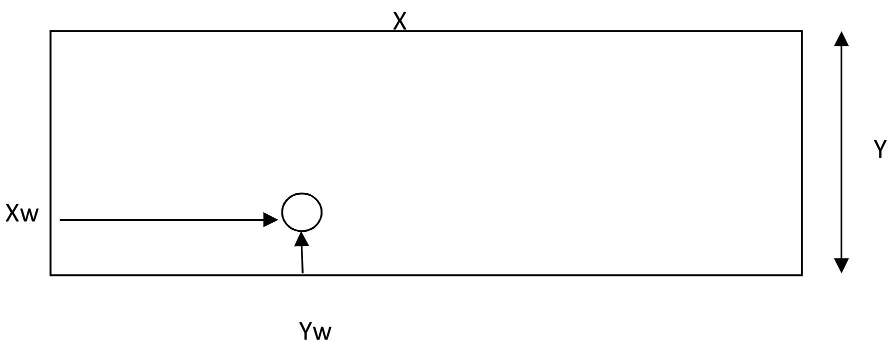

Figure 5. Sketch of a rectangular reservoir, where the well is situated at distances Xw and Yw from the barriers.

6 Analysis of corrected pressure data

The downhole gauge pressures have been matched with above described model. Fig-6 shows the match of the final build-up, both for pressure and for the derivative of the pressure. The pressure derivative displays more information than the pressure and is therefore used to draw conclusions about the reservoir geometry and the presence of flow barriers.
NB: The (Agarwal) effective time is used in order to obtain a straight-line Horner plot for this test with a short and varying rate history and a relatively long build-up. The total build-up time in this figure is 23.5 hrs, with a final effective time of less than 6.

The double wellbore storage behaviour as displayed on the left hand side in Fig-6 is seen in all hot-water wells and is thought to be caused by the “water-hammer” effect: The kinetic energy of the flowing water is abruptly changed into the potential energy of the water level in the annulus, rising above the static water level, compressing the gas present in the top of the annulus. By applying an increasing wellbore storage in the model, this water-hammer effect can be approximated. But in order to get the best match with the more relevant late build-up data (on the right hand side of Fig-7), a non-optimal match of this early wellbore storage has been accepted. The late build-up points were given a higher weight-factor.

Following the moderately accurate match of the initial build-up, caused by these wellbore effects the match of the data after 0.1 hour is good. The late build-up, after 0.8 hour effective time, is influenced by the presence of one flow barrier at approximately 370 m from the well.

Fig-7 presents the model match with the whole test, including all flow periods, on a linear time scale.
The late build-up is presented on the large right-hand scale. This enlarged model match shows that, in spite of all corrections to the pressure data, the model pressures increase somewhat faster than the observed pressures. This may indicate that the barrier is possibly not fully sealing. See Figure 1.

The selection of the preferred model should also be based on seismic and sedimentological information, the top structure map is shown in Fig 1. On the top structure map the faults run in a NW-SE direction and the nearest fault to the well (visible on seismic) is about 500m away to the north-east.

The resulting model parameters demonstrated a good model match with a permeability of 800 mD for the main Delft sandstone, a static reservoir pressure of 240.6 bara (at 2375 mtv) and a relatively low total skin of 0.8 at the final, high, flow rate. The Productivity Index after 34 hrs is about 21 m3/hr/bar.

The skin value has been determined at all flow periods, by matching the same model on all final flowing pressures:

Flow rate (m3/hr):	219	288	388	450	215	281	363
Skin :	1.08	0.83	1.32*	1.04	0.48	0.68	0.81

*) This is a short period of increasing rate. The average rate on which this skin is based is thus too low for the actual rate at the end of this period.

These skin values indicate that the well was still cleaning-up during the first four flow periods with a declining skin at increasing rate, but stabilised during the highest rate at 450 /hr.
The flowrate dependency of the skin is caused by friction over the vertical flow conduit and possibly by the holes in the sand-protection screens.
Extrapolation of the three final skin values (0.48, 0.68 and 0.81) to zero rate results in a real damage skin of only 0.02. The rate dependent skin is thus 0.79 / 363, or 0.0022 hr/m3.

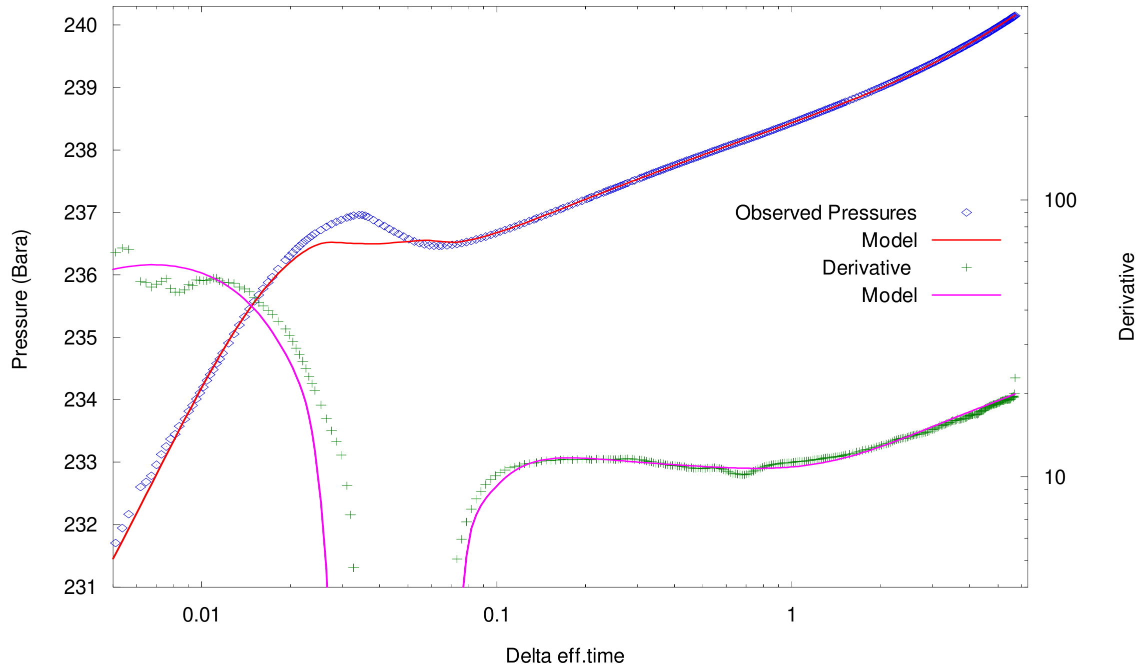

Figure 6- Comparison of measured and modelled Pressure response for Pressure (in bar) and Derivative, showing a good match between the model and the measured data.

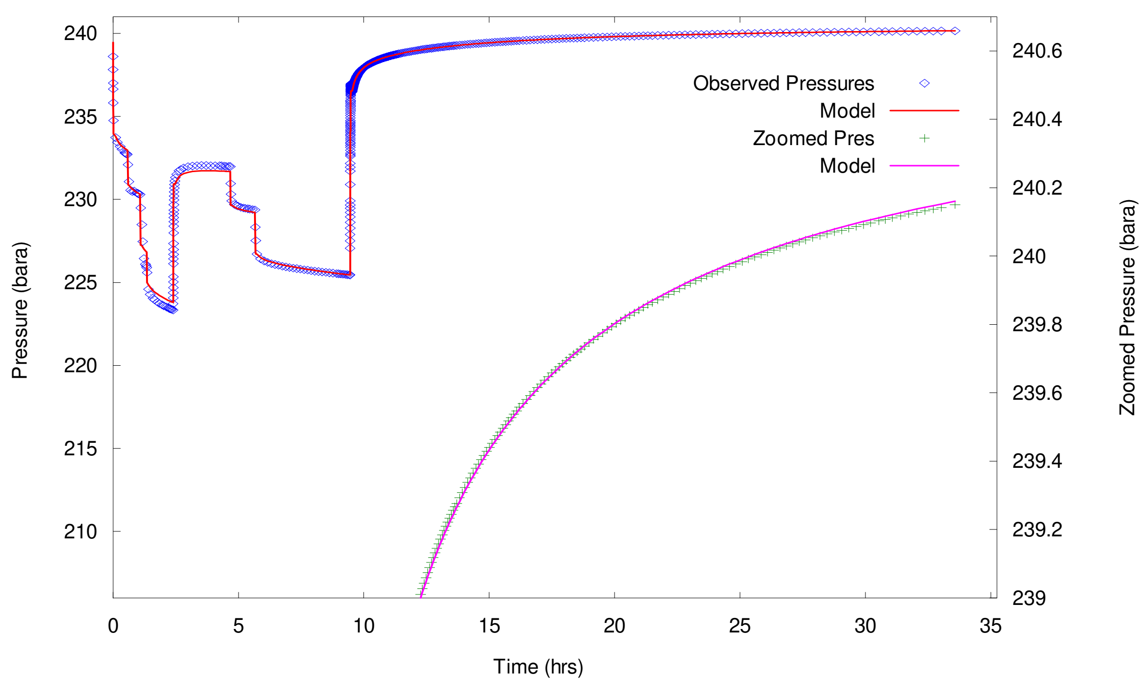

Figure 7 - Comparing the pressure (in bar) response of matched model with measured pressures over full test period.

7 Conclusions and Recommendations

The second Naaldwijk well test has been successful in establishing an accurate estimate of reservoir permeability of about 800 mD, and demonstrates that there is a very low formation skin factor of only 0.02, indicating that there is no formation damage. The rate-dependent skin, caused by friction in the vertical flow conduit, is 0.0022 hr/m^3.

The reservoir pressure (240.6 bar at 2375 mtv) and temperature (87.5 °C) are in line with expectations.

The (transient 34 hrs) PI of the well is high at 21 m3/hr/bar and suggests that a successful geothermal project can be envisaged using the NLW-GT-02 well and the first tested well of the doublet, NLW-GT-01.

There appears to be one flow barrier near the well at a distance of about 370 m from the well, which may be the boundary fault to the north-east (see Figure 1).

Only the Delft sandstone was produced in NLW-GT-02, whereas in NLW-GT-01 also the Alblasserdam sandstone was produced. This may explain the slightly higher salinity of 130 kg/m3 observed in NLW-GT-02 compared to the 120 kg/m3 seen in NLW-GT-01.

A better definition of the boundaries around this doublet and the long-term steady-state PI will be obtained from the results of the ongoing interference test.

8 Appendix.

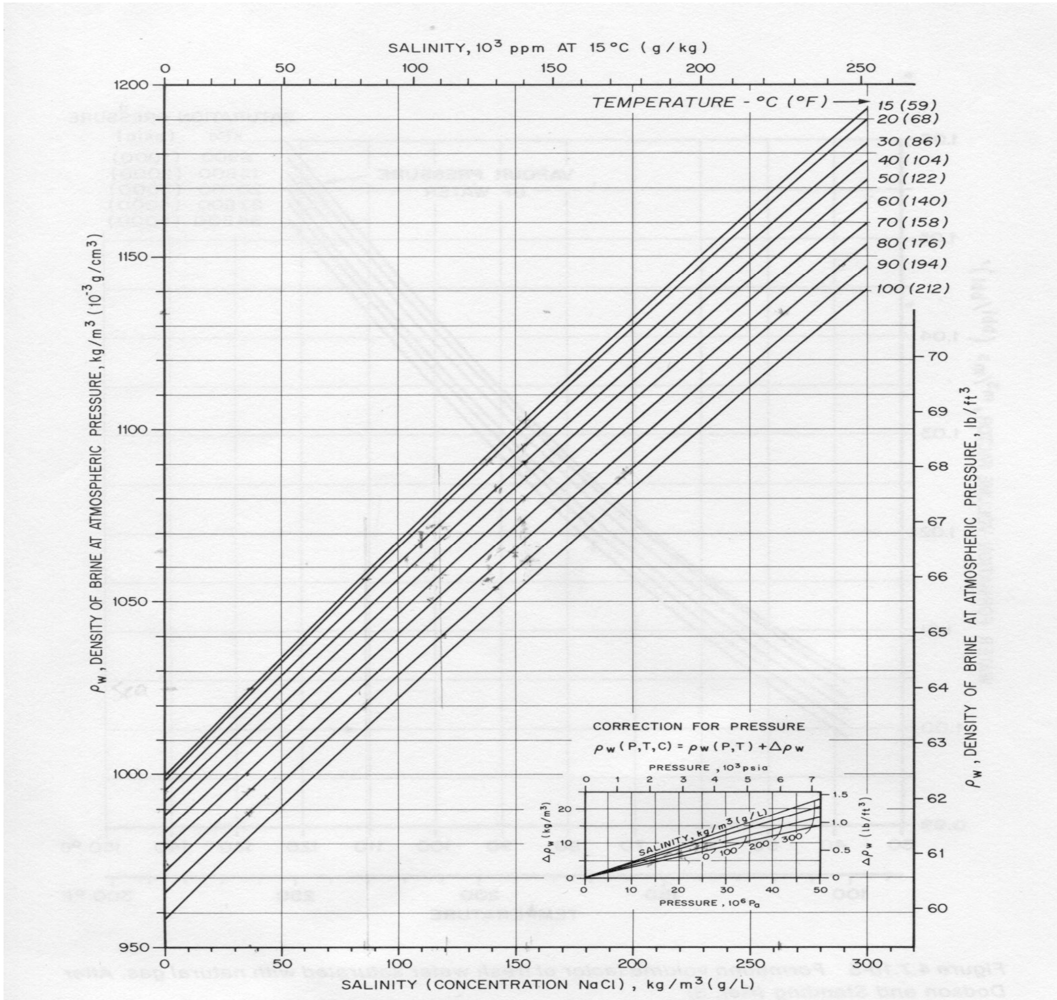

Figure 4.7.10-6 Water density as function of dissolved solids. After Long and Chierici (Ref. 35)

Appendix 1. Water density as function of Salinity